JOURNAL OF VIROLOGY, Apr. 2009, p. 3770–3777 Vol. 83, No. 8
0022-538X/09/$08.00+0 doi:10.1128/JVI.00265-08

Site of Human Rhinovirus RNA Uncoating Revealed by Fluorescent In Situ Hybridization▽

Marianne Brabec-Zaruba,[1] Beatrix Pfanzagl,[1] Dieter Blaas,[2] and Renate Fuchs[1]*

Department of Pathophysiology, Center for Physiology, Pathophysiology and Immunology, Medical University of Vienna, Waehringer Guertel 18-20, A-1090, Vienna, Austria,[1] and Max F. Perutz Laboratories, University Departments at the Vienna Biocenter, Department of Medical Biochemistry, Medical University of Vienna, Dr. Bohr Gasse 9/3, A-1030 Vienna, Austria[2]

Received 5 February 2008/Accepted 9 January 2009

By using fluorescent in situ hybridization (FISH), we visualized viral RNA of human rhinovirus type 2 (HRV2) during its entry into HeLa cells. RNA uncoating of HRV2 is entirely dependent on low endosomal pH (≤5.6). When internalized into cells treated with bafilomycin, which results in neutralization of the endosomal pH, no FISH signal was recorded, whereas in the absence of the drug, fluorescent dots were seen. Therefore, FISH detects the genomic viral RNA only upon its release from the capsid. Free viral RNA was first seen at 10 min postinfection (p.i.) in the perinuclear area of the cell, which is indicative of RNA release in/from late endosomal compartments. Pulse-chase experiments and observation of HRV2 RNA and capsid proteins via microscopy, Western blotting, and reverse transcription-PCR revealed that the RNA signal persisted whereas the protein signal disappeared. This demonstrates transport of capsids to lysosomes and degradation. In contrast, viral RNA that had already been transferred into the cytoplasm escaped lysosomal breakdown as indicated by a persistent FISH signal. Taken together, our results demonstrate by direct means RNA arrival in the cytosol within 10 min p.i. Based on persistence of the FISH signal and productive infection in the presence of the microtubule-depolymerizing drug nocodazole, we localized this process to endosomal carrier vesicles/late endosomes.

Human rhinoviruses (HRVs) are a major cause of the common cold. As *Picornaviridae*, they are nonenveloped with an icosahedral capsid assembled from 60 copies each of four proteins (VP1 through VP4) that encases a single-stranded positive-sense RNA genome (for a review of picornaviruses, see reference 28). The 99 currently characterized HRV serotypes are phylogenetically divided into two species; 73 are HRV-A, and 26 are HRV-B (17). Twelve serotypes of species A (the minor group) use members of the low-density lipoprotein receptor (LDLR) family for attachment. The remaining 87 types (the major group, including representatives of both species) infect via intercellular adhesion molecule 1 (ICAM-1) (31). As demonstrated for a few HRV types, the entry and uncoating pathways of minor and major group viruses differ considerably (1, 22).

As most of the data on minor group virus entry and uncoating have been obtained for HRV type 2 (HRV2) (6, 23, 24), this type was used in all experiments described in the present report. Virus internalization by receptor-mediated endocytosis via LDLR and LDLR-related protein (14, 19) results in virus-receptor dissociation in the mildly acidic pH of early endosomes; the receptors are then recycled and the virus is directed, via endosomal carrier vesicles (ECV) and late endosomes, toward lysosomes (2, 4). As soon as the endosomal pH reaches a threshold pH of ≤5.6, structural changes lead to release of the innermost capsid protein VP4 and to exposure of the amphipathic N terminus of VP1. This presumably results in insertion into the membrane and formation of a pore enabling RNA translocation into the cytoplasm (6, 24, 27). Synthesis of viral proteins is then initiated and followed by genome replication. Finally, progeny viruses are assembled and released from the host cell.

Genome transfer of nonenveloped viruses into the cytosol is still enigmatic and poorly understood. A principal question is whether the virus enters as an entity or whether the genome alone accesses the cytoplasm, presumably through a pore. Previous biochemical data from our groups strongly suggested the latter model, but definitive proof is still lacking. Except for lysosomal degradation of radiolabeled genomic HRV2 RNA (18), the fate of the viral RNA per se during entry and uncoating has not been investigated so far. For picornaviruses in general, few data are available on localization of the viral RNA in the early phase of infection. Only a recent investigation by Bradenburg et al. (7) employing poliovirus labeled with different fluorophores in its protein and RNA demonstrated, by live cell imaging, rapid release of the RNA from vesicles in proximity (100 to 200 nm) to the plasma membrane. However, this technique allows only for colocalization of protein and RNA; once the RNA has left the virion, its signal is lost. Therefore, here we used another method allowing for visualization of viral RNA, fluorescent in situ hybridization (FISH). This technique allows for detection of poliovirus RNA during replication (12), but at 0.5 h postinfection (p.i.), the earliest time point of observation, small dots at the cell periphery presumably representing the input RNA were also seen (10). Therefore, we assessed whether FISH allowed visualization of HRV2 RNA during entry and uncoating. We show here that free RNA is

* Corresponding author. Mailing address: Department of Pathophysiology, Center for Physiology, Pathophysiology and Immunology, Medical University of Vienna, Waehringer Guertel 18-20, A-1090, Vienna, Austria. Phone: 431 40400 5127. Fax: 431 404005130. E-mail: renate.fuchs@meduniwien.ac.at.

▽ Published ahead of print on 21 January 2009.

first detected at between 10 and 12 min after virus internalization. Using various drugs that block distinct endocytic transport steps, we demonstrated that RNA release into the cytoplasm occurs from ECV in the perinuclear area. De novo-synthesized protein and RNA were seen at 3.5 h and 6.5 h p.i. as an endoplasmic reticulum-like pattern even when microtubules were depolymerized with nocodazole.

MATERIALS AND METHODS

Chemicals. All chemicals were obtained from Sigma (St. Louis, MO) unless specified otherwise. Bafilomycin A1 (Alexis Corp., Lausen, Switzerland), nocodazole, and wortmannin, were dissolved in dimethyl sulfoxide at 20 mM, 20 mM, and 40 μM, respectively, and stored at −20°C.

Cells, buffers, and media. HeLa-H1 (HeLa) cells were grown in minimal essential tissue culture medium (MEM) supplemented with 10% heat-inactivated fetal calf serum, 2 mM L-glutamine, 100 units/ml penicillin G sodium salt, and 100 μg/ml streptomycin sulfate (all from Gibco Invitrogen Corp., Paisley, United Kingdom). HRV2, originally obtained from the ATCC, was propagated in HeLa cells, and the titer was determined as 50% tissue culture infectious dose ($TCID_{50}$) (3).

Internalization of HRV2. HeLa cells were grown on coverslips until half confluent and preincubated in serum-free MEM for 30 min at 34°C. Where indicated, 200 nM bafilomycin, 100 nM wortmannin, or 20 μM nocodazole (all final concentrations) was present. HRV2 at a multiplicity of infection (MOI) of 150 (i.e., ~150 PFU/cell and ~1,500 $TCID_{50}$/cell as determined by comparison of both techniques) was internalized for 5, 10, and 12 min in fresh MEM (with or without the respective drug) at 34°C. Cells were washed twice with phosphate-buffered saline (PBS), fixed with 4% paraformaldehyde (PFA) in PBS at 4°C for 10 min, and prepared for indirect immunofluorescence microscopy or FISH. For pulse-chase experiments, virus was internalized for 12 min, nonattached virus was washed away with PBS containing 1 mM $CaCl_2$ and 1 mM $MgCl_2$, and the cells were further incubated in MEM. Prior to RNA isolation and Western blotting, they were briefly rinsed with PBS–1 mM EDTA.

Immunofluorescence microscopy. After fixation with PFA, cells were permeabilized with PBS containing 4% PFA and 0.2% Triton X-100 for 10 min. Samples were then quenched with 50 mM NH_4Cl in PBS. Blocking was performed with 10% goat serum in PBS (blocking buffer). HRV2 was detected with the monoclonal antibody 8F5 (10 μg/ml) directed against the viral capsid protein VP2 (30), followed by Alexa 488-labeled goat anti-mouse immunoglobulin G (IgG) (1:1,000; Molecular Probes, Inc., Eugene, OR). First and second antibodies were diluted in blocking buffer; incubation was for 40 min at room temperature. Nuclei were stained with Hoechst dye 33342. Cells were mounted in a 9:1 (vol/vol) mixture of glycerol and 1 M Tris-HCl (pH 8.6) containing 25% diazabicyclo(2.2.2)octane (Merck, Darmstadt, Germany). Cells were viewed under a Zeiss Axioplan 2 fluorescence microscope using Axiovision software.

Preparation of the fluorescent riboprobe. For plus-strand RNA detection, a riboprobe of minus polarity was prepared as described previously (12). In short, a cDNA fragment including bp 11 to 7102 from HRV2 was restricted from the infectious HRV2 cDNA clone (9) by KpnI and BamHI digestion. Using 5′-AAC ATA ATG ATT GAA GAA GAC AGA CGG AG-3′ (p1) and 5′-TAG TTG GGT AAC TGT ATT TAA GCA TTC TAG CCG-3′ (p2) as primers, the sequence corresponding to nucleotides 4772 to 5558 was amplified. In a next amplification step, the T7 promoter sequence (underlined) was added to the coding strand by using 5′-ATT AAT ACG ACT CAC TAT AGG GTA ACT GTA T-3′ instead of p2. Finally, the riboprobe was generated by in vitro transcription with T7 polymerase in the presence of fluorescein isothiocyanate (FITC)-UTP (Boehringer) as described in detail previously (12). Briefly, 200 ng template DNA; 1 mM ATP, GTP, and CTP; 0.65 mM UTP; 0.35 mM FITC-UTP; and 50 U RNase inhibitor were incubated in transcription buffer (final volume, 50 μl) with 50 U T7 polymerase for 2 h at 37°C. Unincorporated nucleoside triphosphates were removed with a Micro Bio-Spin 6 column (Bio-Rad, Hercules, CA). To ensure penetration of the probe into the fixed and permeabilized cells, the fluorescent RNA was subjected to alkaline hydrolysis at 60°C for 80 min, generating fragments of approximately 100 nucleotides in length. Oligonucleotides of less than 20 bases were removed on a Bio-Spin 30 column. Lengths of the fragments and fluorescence labeling were verified by Northern blotting (12).

FISH. Cells were fixed, permeabilized, and quenched as described for immunofluorescence, using RNase-free solutions. The riboprobe was dissolved in water, diluted 1:10 in hybridization buffer (50% formamide, 10 mM Tris-HCl [pH 7.4], 600 mM NaCl, 10% dextran sulfate, 10 mM dithiothreitol, 0.05% bovine serum albumin, 0.1% sodium dodecyl sulfate [SDS], 200 μg salmon sperm DNA, and 100 μg yeast tRNA per ml) (12), and hybridized to the cells at 40°C for 8 h. After four washes in 0.1% SSC (1% SSC is 150 mM NaCl and 15 mM sodium citrate) for 10 min, the slides were mounted in an RNase-free mounting medium as described above and stored at 4°C overnight prior to viewing.

Reverse transcription-PCR (RT-PCR) of viral RNA. Total RNA was isolated from semiconfluent cells grown in one well of a 12-well tissue culture plate using peqGOLD TriFast (peqlab Biotechnologie GmbH, Germany) as recommended by the manufacturer. RNA was dissolved in 40 μl water, and synthesis of cDNA with murine leukemia virus reverse transcriptase (Fermentas, Vilnius, Lithuania) was primed with random hexamers (Invitrogen, Carlsbad, CA) and carried out in the presence of RiboLock RNase inhibitor (Fermentas). The reaction mixture (12 μl) containing 2 μl of this RNA was incubated for 10 min at room temperature followed by 60 min at 37°C. The enzyme was then heat inactivated for 10 min at 70°C. Because of the large excess of HRV2 cDNA over β-actin cDNA resulting from the respective RNA concentrations in the sample, PCRs were carried out separately for HRV2 and β-actin to avoid competition (20). The samples were diluted 1:10, and 1 μl each was amplified in a final volume of 25 μl containing 0.05 μM primers either for β-actin (5′-ATC TGG CAC CAC ACC TTC TAC AAT GAG CTG CG-3′ [forward] and 5′-CGT CAT ACT CCT GCT TGC TGA TCC ACA TCT GC-3′ [reverse]) or for HRV2 (5′-CCA ATA GCC GGT AAT CAG CC-3′ [forward] and 5′-GCA CCA TTT GAA GCA GCA TC-3′ [reverse]), 0.2 mM deoxynucleoside triphosphates, and 0.04 unit GoTaq polymerase (Promega, Madison, WI) in Green GoTaq reaction buffer for 24 cycles. It was ascertained that the reaction was still in the linear phase when terminated. Cycling conditions were 0.5 min at 94°C, 1 min at 60°C, and 1 min at 72°C. Equal volumes of the PCR products of HRV2 and β-actin amplification reactions were mixed, electrophoresed through 1.5% agarose gels, stained with ethidium bromide, and photographed under UV light.

Western blotting for HRV2 VP1. Semiconfluent cells grown in a well of a 24-well tissue culture plate were lysed in 100 μl reducing SDS-polyacrylamide gel electrophoresis sample buffer, heated for 7 min at 95°C, and centrifuged for 5 min at 15,000 × *g*. Twenty microliters of the supernatant was run on an SDS-12% polyacrylamide gel, and proteins were transferred by semidry blotting onto a polyvinylidene fluoride membrane. The membrane was blocked with 3% milk powder in PBS (blocking buffer) and incubated with rabbit antiserum raised against a peptide corresponding to the 24 N-terminal residues of HRV2 VP1 (diluted 1:400 in blocking buffer containing 0.2% Tween 20). Blots were washed, and bound antibody was detected with horseradish peroxidase-coupled goat anti-rabbit IgG (Sigma; diluted 1:20,000) in the same buffer but containing 0.05% Tween 20, followed by SuperSignal West Pico chemiluminescent substrate (Pierce, Rockford, IL).

Quantification of degradation of viral RNA and protein. Images from the gel-resolved RT-PCR products and from the X-ray films exposed to chemiluminescence from the Western blots were scanned. The bands corresponding to HRV2-specific DNA were normalized to the respective control actin bands and related to the amount present in the cells after the 12-min pulse. The antiserum against the N terminus of VP1 also recognized a protein present in the cells migrating slightly above VP1. This band was taken as an internal control. Intact VP1 present after the 12-min pulse was set to 100%.

RESULTS

Endocytosis of HRV2 is very fast; after uptake via coated or uncoated vesicles, the virus arrives in early endosomes within the first 5 min (6). Shortly after, it reaches late acidic compartments where structural modifications of the viral capsid can be detected by using a conformation-specific monoclonal antibody. This transition from the native virion to empty capsids occurs at around 10 min p.i., as previously shown by immunoprecipitation from purified endosomes (23). We thus asked whether we could specifically detect RNA from the incoming virus as soon as it was released.

Free viral RNA is detected by the fluorescent RNA probe, but encapsidated RNA is not. Bafilomycin completely prevents the acid-induced conformational change of the viral capsid; consequently, RNA uncoating does not take place (2). Therefore, this drug was used to investigate whether our probe

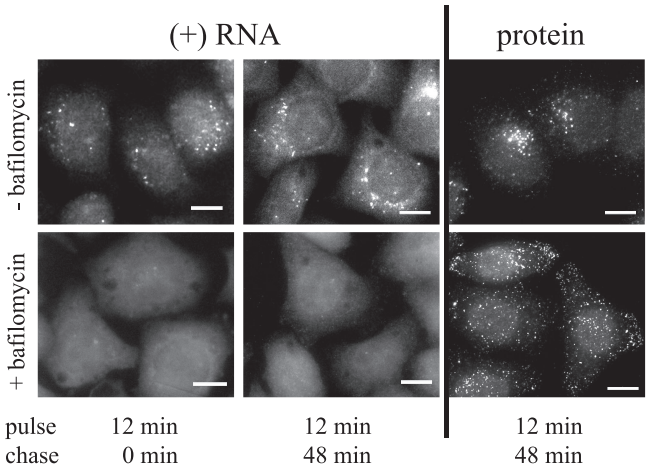

FIG. 1. Uncoated HRV2 RNA is detected by FISH. HeLa cells were preincubated without (upper panels) or with (lower panels) 200 nM bafilomycin for 30 min, and HRV2 was internalized at 1,500 $TCID_{50}$/cell for 12 min (with or without) at 34°C (pulse). Cells were washed and further incubated for the times shown (chase). After fixation, input RNA was detected with a riboprobe containing FITC-labeled UTP (left and middle panels), and viral capsid protein was visualized by indirect immunofluorescence using the monoclonal antibody 8F5 followed by Alexa Fluor 488-labeled goat anti-mouse IgG (right panels). Cells were viewed under a Zeiss Axioplan 2 fluorescence microscope. Bars, 10 μm.

hybridizes with encapsidated and/or uncoated viral RNA. HeLa cells were preincubated without or with bafilomycin, HRV2 was internalized for 12 min, and the cells were fixed either immediately or after further incubation for another 48 min; they were then either processed for FISH or stained for viral proteins. As depicted in Fig. 1, a clear FISH signal was seen in both samples in the absence of bafilomycin, whereas no signal was evident in cells treated with the drug (lower left and middle panels); even at 17 h p.i. in the presence of bafilomycin, no signal was detected (not shown). Staining for viral protein clearly showed that HRV2 was internalized (right panels). However, as bafilomycin not only inhibits endosome acidification but also blocks the budding of ECV from early endosomes, the internalized virus remains in peripheral early compartments (2). The absence of RNA staining in the presence of bafilomycin demonstrates that RNA within the capsid is inaccessible to the probe; this makes it an excellent tool for the observation of the uncoated viral genome.

Free viral RNA remains in the cytoplasm, but the viral capsid progresses to lysosomes. We next asked whether the free RNA released from the incoming virus would be transferred to and remain in the cytosol. To this end, we took advantage of HRV2 transport to lysosomes; empty capsids and virus that has failed to uncoat arrive in lysosomes at about 25 min after uptake, where viral proteins and RNA are rapidly degraded (18, 23) (see Fig. 5 for a time course of HRV2 through endocytic compartments). Therefore, HRV2 was internalized for 12 min, and cells were further incubated in the absence of virus (chase) for 18, 48, and 108 min. A time-dependent decrease in stained viral proteins was seen following pulse internalization for 12 min. The fluorescence signal had virtually disappeared at a chase of 108 min (Fig. 2, upper panels). This indicates that the viral proteins had been almost completely degraded. Under these conditions, de novo viral protein synthesis is not yet detectable (see below). Cells infected by the same protocol were also stained for RNA. In contrast to the gradual decrease in fluorescence staining of viral proteins during the chase, the FISH signal persisted (Fig. 2, lower panels).

In addition, we also analyzed the degradation of viral protein and RNA by Western blotting and RT-PCR. Following the same protocol as described above, virus was internalized and chased for the times indicated in Fig. 3. Samples were subjected to SDS-polyacrylamide gel electrophoresis followed by detection of VP1 via a rabbit antiserum raised against the N-terminal 24 amino acid residues, a sequence that becomes exposed upon the conformational transition to subviral particles and is therefore particularly prone to digestion (16). Nevertheless, all viral proteins as well as the RNA are rapidly

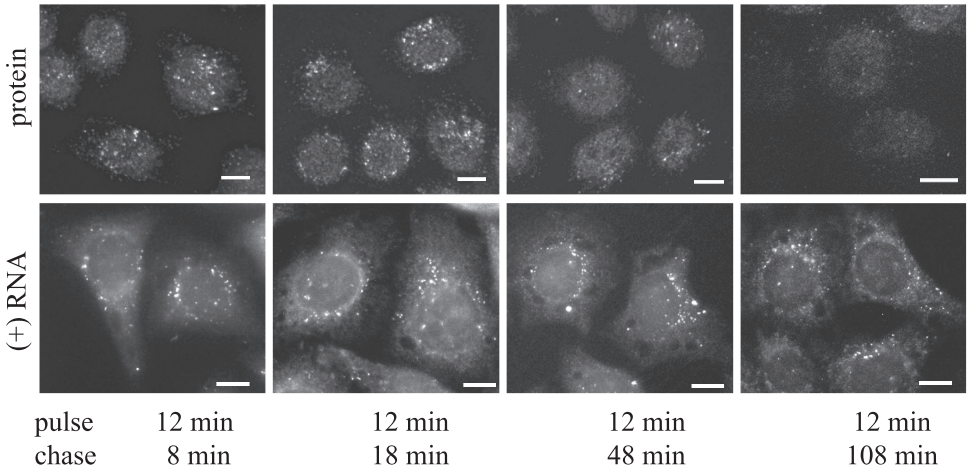

FIG. 2. Viral input RNA is still detected after lysosomal degradation of viral protein. HRV2 at 1,500 $TCID_{50}$/cell was internalized for 12 min at 34°C. Cells were washed and further incubated in fresh medium for the times indicated (chase). Cells were fixed, and viral protein (upper panels) and uncoated RNA (lower panels) were then detected by immunofluorescence and FISH as detailed in the legend to Fig. 1. Note the strong decay of the signal of viral protein, which is due to lysosomal degradation, while the FISH signal is maintained. Bars, 10 μm.

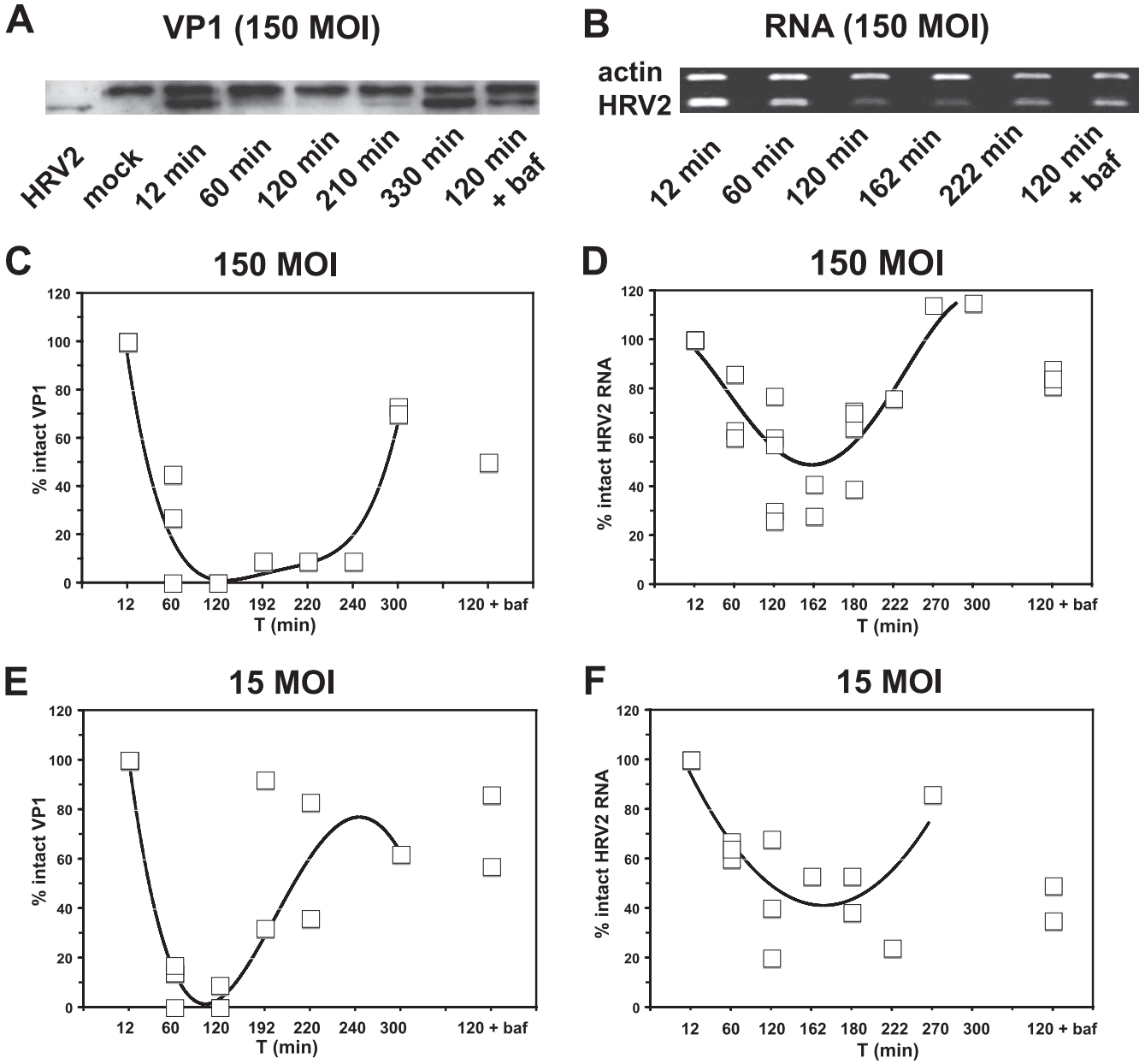

FIG. 3. Input viral protein and RNA are degraded to different extents. HRV2 at MOIs of 15 and 150 was internalized into HeLa cells for 12 min (pulse). Cells were washed, and incubation was continued for the times indicated (pulse plus chase). As controls, cells were preincubated with 200 nM bafilomycin for 30 min, and the drug was present throughout the experiment. (A) Cells were lysed and proteins were separated on an SDS-12% polyacrylamide gel, followed by Western blotting with an antibody recognizing N-terminal sequences of VP1. Only the part of the gel showing intact VP1 is depicted. The unspecific protein band also seen in the absence of virus was taken as an internal loading control. (B) Total RNA was extracted and transcribed into cDNA, and β-actin and viral RNA sequences were amplified separately within the linear range and mixed in equal amounts for agarose gel electrophoresis. (C to F) For quantification, the gels were scanned and the viral bands were related to the internal controls and expressed as percentages of the amount at 12 min p.i. Data from three to six individual experiments for each setup and the polynominal fourth-order trendlines are shown.

degraded to trichloroacetic acid-soluble products once they arrive in lysosomes (13, 15, 18, 26). In a parallel experiment, total RNA was reverse transcribed, and the amount of viral plus-strand RNA relative to β-actin mRNA was determined by PCR. Figure 3 shows a representative Western blot of VP1 (Fig. 3A) and an ethidium bromide-stained agarose gel of the amplified cDNAs (Fig. 3B). The band of VP1 obtained immediately after internalization (12-min pulse and 0-min chase) quickly decreased up to 108 min (i.e., 120 min p.i.), when all VP1 had disappeared (Fig. 3A). The band then reappeared, and its intensity increased again with time because of de novo synthesis. Viral RNA also decreased but never disappeared, and the lowest level attained was roughly 30% of the input (12-min pulse and 108-min chase) (Fig. 3B). Here also an

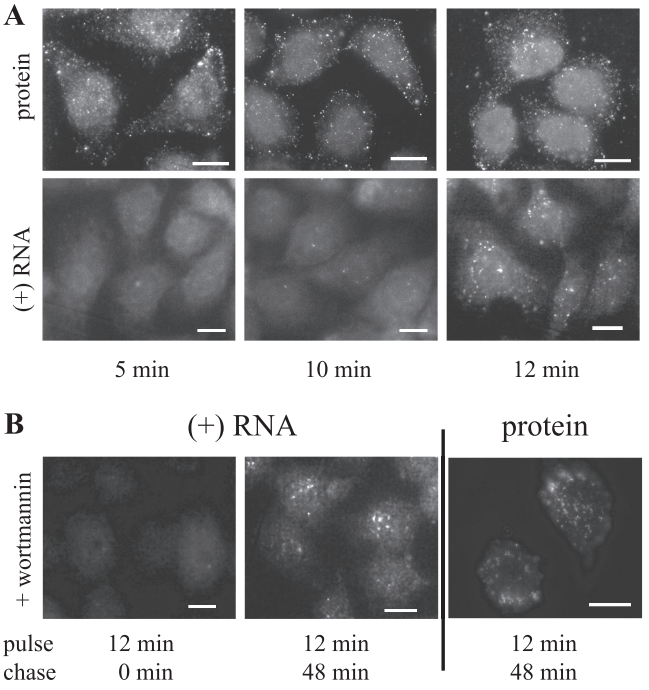

FIG. 4. Time course of RNA release into the cytoplasm correlates with arrival in late endosomes. (A) HeLa cells were infected with HRV2 at 1,500 $TCID_{50}$/cell for the times indicated. After fixation, immunofluorescence detection of viral protein (upper panels) and FISH (lower panels) were performed. Bars, 10 μm. (B) HeLa cells were preincubated with or withoug100 nM wortmannin, virus was internalized as for panel A, and cells were either immediately fixed after internalization (12 min) or further incubated in the absence of virus for 48 min. Wortmannin was always present during the experiment. Left two panels, FISH; right panel, immunofluorescence. Bars, 10 μm.

increase is evident at later times, which is due to replication. As expected, lysosomal degradation was prevented by bafilomycin in both cases (Fig. 3A and B). The same experiments were also carried out with an MOI of 15 with essentially the same result. The individual experiments are summarized in the form of graphs in Fig. 3C to F. These results demonstrate that a large part of the RNA, as detected by FISH, has been released from the endosomes into the cytosol and did not arrive in lysosomes as did the capsid proteins. Furthermore, as the FISH signal remained roughly the same between 60 min (12-min pulse and 48-min chase) and 120 min (12-min pulse and 108-min chase) (Fig. 2), the viral RNA is apparently not degraded by cytoplasmic RNases (15, 26).

RNA release into the cytoplasm correlates with virus arrival in late endosomes. To pinpoint the site of RNA release, virus was internalized for 5, 10, and 12 min. An aliquot of the cells was fixed and stained for HRV2 proteins. As shown in Fig. 4A, viral capsid protein is clearly visible at 5 min p.i. At this time, virus is present mainly in peripheral vesicles and at the plasma membrane. At 10 and 12 min, viral protein is seen in endosomes close to the nucleus that had been identified as late endosomes by fractionation experiments and colocalization studies (2, 23). The other aliquot of the cells was processed for FISH; the results are depicted in the lower panels of Fig. 4A. The FISH signal and virus-specific antibody staining exhibit distinct kinetics of appearance: although internalized viral protein was evident at each time point, no RNA staining was seen at 5 min after internalization, a faint signal was seen at 10 min, and a strong signal appeared at 12 min. This is again evidence for the RNA being released in a time-dependent manner.

RNA release is delayed by wortmannin and unaffected by disruption of microtubules. As shown recently, the phosphatidylinositol 3-kinase inhibitor wortmannin does not affect virus internalization but leads to a delay in transport from early to late endosomes, in virus uncoating, in lysosomal degradation of the capsid proteins, and in HRV2 de novo synthesis (5). Therefore, we examined the effect of wortmannin on RNA uncoating via FISH by using a pulse-chase protocol similar to that used for Fig. 2. Indeed, in the presence of the drug, no RNA staining was seen at 12 min after internalization (compare Fig. 4B with A), but it was clearly visible at 60 min, when the virus still localized to peripheral enlarged endosomes (Fig. 4B, left panel). This is in line with RNA release being delayed by wortmannin, an effect also seen for productive uncoating and infection (5).

As shown previously, disruption of microtubules by nocodazole results in accumulation of the virus in ECV, intermediates between early and late endosomes that preferentially localize to the cell periphery. Conformational change and de novo viral protein synthesis were unaffected by the drug, as these compartments acidify to a pH similar to that of late endosomes. However, protein degradation is prevented, as ECV consequently do not deliver their cargo to lysosomes (2). Therefore, the influence of nocodazole on localization of the incoming RNA and the synthesis of new genomic RNA was studied. As depicted in Fig. 5A (upper panels), at 60 min p.i. viral protein was present in large, more peripheral vesicles, a typical staining pattern resulting from nocodazole treatment (2). Viral RNA preferentially accumulated at one side of the nucleus, whereas it was more disperse and more evenly distributed around the nucleus in the presence of the drug (lower panels). There are subtle differences in the staining patterns of RNA and viral capsids in the presence of nocodazole, supporting the above results on separation of the two viral constituents upon uncoating. At 222 min p.i. (i.e., 12-min pulse followed by 3.5-h chase) (Fig. 5B), viral de novo synthesis was apparent regardless of the presence of nocodazole. At 6.5 h, de novo-generated viral protein and viral RNA (Fig. 5C) gave rise to a staining pattern reminiscent of the endoplasmic reticulum (11; M. Brabec-Zaruba et al., unpublished data). This is in contrast to the case for poliovirus, where at 3.5 h p.i. newly synthesized nonstructural protein 2B and plus-strand RNA were dispersed in the cytoplasm in nocodazole-treated cells. Nevertheless, neither production of virus progeny by poliovirus nor that by HRV2 is inhibited by nocodazole treatment (2, 11).

DISCUSSION

Using FISH for detection of plus-strand viral RNA and indirect immunofluorescence microscopy for detection of viral protein, we investigated the site of viral RNA uncoating. This was possible because the generated riboprobe did not hybridize with viral RNA as long as it remained within the intact capsid. This was inferred from the absence of the signal in the presence of bafilomycin, i.e., under conditions where the conformational change and RNA release do not occur. The RNA

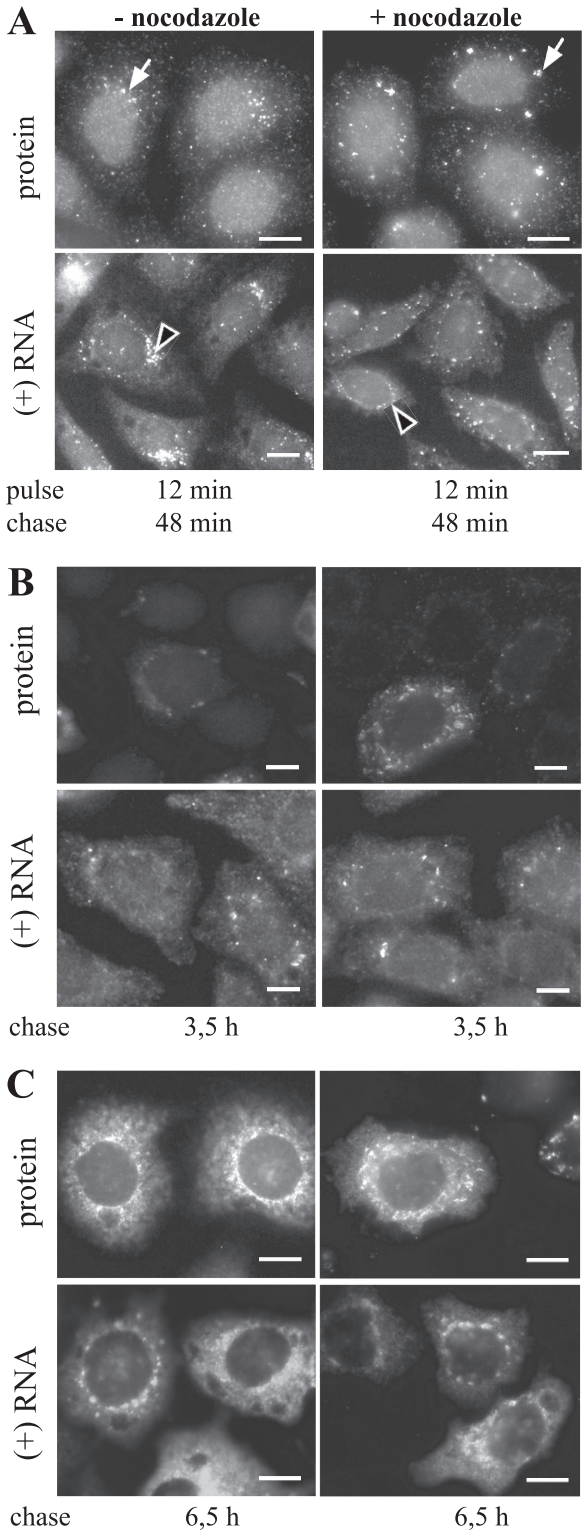

FIG. 5. Effect of nocodazole on RNA release and de novo synthesis of HRV2. Where indicated, HeLa cells were preincubated with 20 μM nocodazole for 30 min. Virus was then internalized for 12 min (with or without nocodazole) as for Fig. 2, followed by additional incubation with or without nocodazole for 48 min (A), 210 min (B), and 390 min (C), and cells were processed for separate detection of viral protein and RNA. In the absence of the drug, HRV2 proteins were present in perinuclear vesicles (A, top left panel) (arrow) compared to the large peripheral vesicles seen in the presence of nocodazole (A, top right panel) (arrow). RNA preferentially accumulated on one side of the nucleus (A, bottom left panel) (arrowhead), whereas it was more dispersed in the presence of the drug (A, bottom right panel) (arrowhead). Bars, 10 μm.

became visible only after uncoating, giving rise to discrete fluorescent dots in the perinuclear area. Furthermore, after degradation of viral protein in lysosomes, the persistence of a strong FISH signal indicated that the RNA had been transferred into the cytosol. Based on the time-dependent progress of HRV2 through endocytic subcompartments (Fig. 6) and the use of drugs that block distinct transport steps as well as productive uncoating and infection (2, 5, 23), the appearance of the FISH signal correlated with virus arrival in late endosomes.

Although by fluorescence microscopy we cannot unequivocally demonstrate that the RNA is indeed in the cytoplasm (and not released into the lumen of the endosome) when the FISH signal appears, this is highly likely for the following reasons. (i) The signal remains in the same area of the cell starting from 10 to 12 min p.i. for up to 108 min; at this time the capsids have already progressed to lysosomes as seen from the disappearance of the protein signal (Fig. 2) due to degradation (23). (ii) The quantification of intact viral RNA and protein (Fig. 3) as a function of time (chase) after internalization (12-min pulse) shows complete disappearance of capsid proteins, while 30% of the input RNA remained intact at 120 min. (iii) The input viral RNA gives rise to bright, relatively large spots with an appearance similar to that of mRNAs encoding cytoplasmic proteins such as glyceraldehydes 3-phosphate dehydrogenase (21). It is of note that poliovirus RNA detected with FISH early after infection (0.5 to 1.0 h) exhibits similarly discrete spots in the cell periphery that later (1.5 h) give rise to large spots in the perinuclear area (10); as the Hogle group recently demonstrated RNA release into the cytoplasm from peripheral endosomes (7), these spots must be interpreted as stemming from input RNA. (iv) RNA replication that is known to take place on the cytoplasmic side of membranous structures (11, 25) results in an increased FISH signal for poliovirus at >2.5 h p.i (8, 10) as well as for HRV2 at >5.0 h p.i. (Fig. 5C) (Brabec-Zaruba et al., unpublished data). Finally, (v) release of nucleocapsids of Semliki Forest virus after low-pH-induced membrane fusion from endosomes into the cytoplasm gives rise to a grainy but not diffuse cytoplasmic staining pattern (29).

We have been using various reagents known to block distinct steps in the entry pathway in order to assess the correlation between productive uncoating (i.e., giving rise to infection) (2, 5) and RNA release as analyzed via determination of empty capsids. Employing the same drugs, we now analyzed these processes by using FISH. Bafilomycin, which completely blocks uncoating and infection, prevented the appearance of the FISH signal despite viral capsid proteins being detected in endosomes. Wortmannin, previously shown to delay virus transport from early to late endosomes and, as a consequence, viral replication (5), also led to a delay in RNA release. Finally, nocodazole, which depolymerizes microtubules and thus prevents transport of the virus from ECV to late endosomes, did not affect the intensity but affected the pattern of the FISH signal. This indicates that the RNA had been

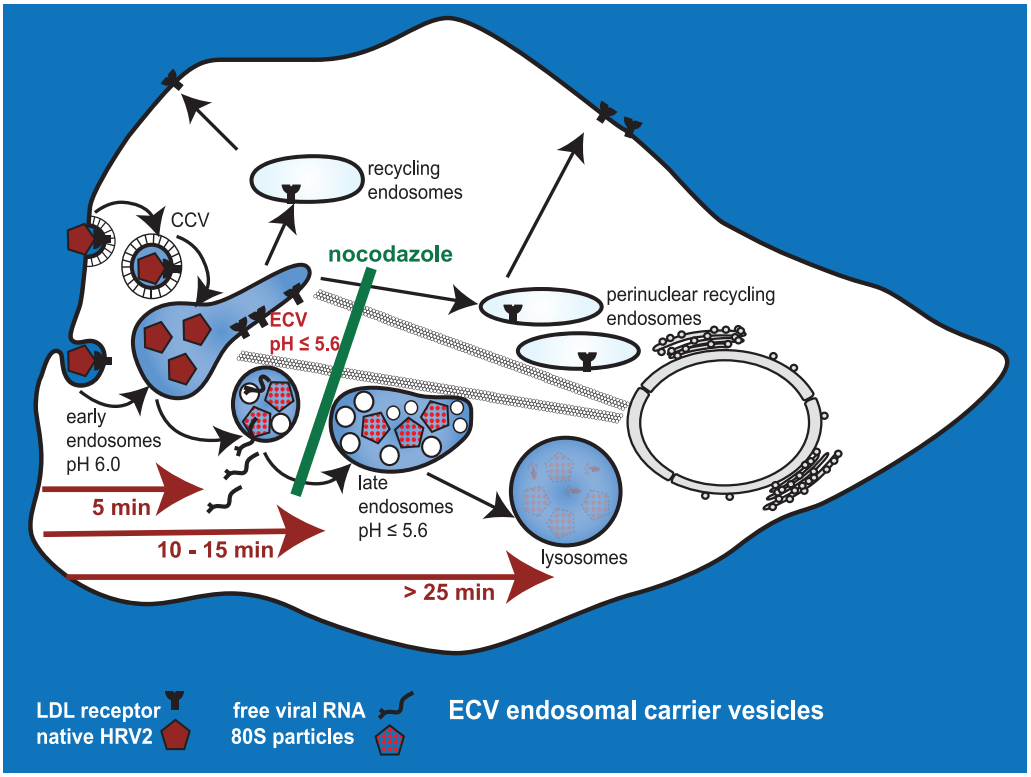

FIG. 6. Kinetics of HRV2 transport through endosomal compartments and RNA release as detected by FISH. HRV2 internalized by clathrin-coated and noncoated vesicles is delivered to early endosomes, where virus is released from its receptors at a pH of ≤6.5. Receptors are recycled to the plasma membrane, and virus is further transferred into ECV, where the lower pH (≤5.6) induces the conformational modification of viral capsid proteins that results in RNA release and RNA transfer into the cytoplasm. Empty capsids and virus that has failed to uncoat are further transported to late endosomes and are finally degraded in lysosomes. Nocodazole does not affect RNA uncoating and its transfer into the cytoplasm but prevents further transport of viral capsids to late endosomes and lysosomes.

released from ECV and correlates with data showing that conformational change of the virion and productive infection occur in the presence of nocodazole (2). However, in contrast to the case for poliovirus, the location of newly synthesized HRV2 protein and RNA at 3.5 h p.i. was unaffected by disruption of microtubules (11).

In summary, we have successfully employed FISH to pinpoint the time p.i. and the site of release of the HRV2 genomic RNA into the cytosol and have correlated the present results with previous data on productive infection using different drugs. The noncovalently RNA-binding fluorescent dye Syto82 has been used to follow poliovirus RNA within the virus up to the point where it is being released from the capsid. Apparently, binding of this dye to poliovirus RNA is dependent on its secondary structure, as the fluorescent signal is lost after uncoating (7). In contrast, FISH, as used here, allows for detection of the HRV2 RNA as soon as it has left the virion. However, neither method can distinguish between the released RNA being still within the endosome (to be further transferred into the cytoplasm) or having already arrived in the cytosol. Notwithstanding, by showing by RT-PCR, Western blotting, FISH, and immunofluorescence microscopy that viral capsid proteins are entirely degraded whereas a substantial part of the viral RNA remains intact, we demonstrate by direct means RNA arrival in the cytosol within a time frame of 10 to 12 min and localize this process to ECV and late endosomes.

ACKNOWLEDGMENTS

We gratefully acknowledge the collaboration with Kurt Bienz and Denise Egger to establish the FISH procedure, and we thank Andrea Glaser for assistance in preparing the riboprobe.

This work was supported by Austrian Science Foundation grant P-17590 to R.F.

REFERENCES

1. **Bayer, N., E. Prchla, M. Schwab, D. Blaas, and R. Fuchs.** 1999. Human rhinovirus HRV14 uncoats from early endosomes in the presence of bafilomycin. FEBS Lett. **463:**175–178.
2. **Bayer, N., D. Schober, E. Prchla, R. F. Murphy, D. Blaas, and R. Fuchs.** 1998. Effect of bafilomycin A1 and nocodazole on endocytic transport in HeLa cells: implications for viral uncoating and infection. J. Virol. **72:**9645–9655.
3. **Blake, K., and S. O'Connell.** 1993. Virus culture, p. 81–122. *In* D. R. Harper (ed.), Virology labfax. Blackwell Scientific Publications, London, United Kingdom.
4. **Brabec, M., G. Baravalle, D. Blaas, and R. Fuchs.** 2003. Conformational changes, plasma membrane penetration, and infection by human rhinovirus type 2: role of receptors and low pH. J. Virol. **77:**5370–5377.
5. **Brabec, M., D. Blaas, and R. Fuchs.** 2006. Wortmannin delays transfer of human rhinovirus serotype 2 to late endocytic compartments. Biochem. Biophys. Res. Commun. **348:**741–749.
6. **Brabec, M., D. Schober, E. Wagner, N. Bayer, R. F. Murphy, D. Blaas, and R. Fuchs.** 2005. Opening of size-selective pores in endosomes during human rhinovirus serotype 2 in vivo uncoating monitored by single-organelle flow analysis. J. Virol. **79:**1008–1016.
7. **Brandenburg, B., L. Y. Lee, M. Lakadamyali, M. J. Rust, X. Zhuang, and J. M. Hogle.** 2007. Imaging poliovirus entry in live cells. PLoS Biol. **5:**e183.
8. **Cui, Z. Q., Z. P. Zhang, X. E. Zhang, J. K. Wen, Y. F. Zhou, and W. H. Xie.** 2005. Visualizing the dynamic behavior of poliovirus plus-strand RNA in living host cells. Nucleic Acids Res. **33:**3245–3252.
9. **Duechler, M., T. Skern, D. Blaas, B. Berger, W. Sommergruber, and E.**

Kuechler. 1989. Human rhinovirus serotype 2: in vitro synthesis of an infectious RNA. Virology **168:**159–161.
10. **Egger, D., and K. Bienz.** 2002. Recombination of poliovirus RNA proceeds in mixed replication complexes originating from distinct replication start sites. J. Virol. **76:**10960–10971.
11. **Egger, D., and K. Bienz.** 2005. Intracellular location and translocation of silent and active poliovirus replication complexes. J. Gen. Virol. **86:**707–718.
12. **Egger, D., R. Bolten, C. Rahner, and K. Bienz.** 1999. Fluorochrome-labeled RNA as a sensitive, strand-specific probe for direct fluorescence in situ hybridization. Histochem. Cell Biol. **111:**319–324.
13. **Helenius, A., J. Kartenbeck, K. Simons, and E. Fries.** 1980. On the entry of Semliki Forest virus into BHK-21 cells. J. Cell Biol. **84:**404–420.
14. **Hofer, F., M. Gruenberger, H. Kowalski, H. Machat, M. Huettinger, E. Kuechler, and D. Blaas.** 1994. Members of the low-density lipoprotein receptor family mediate cell entry of a minor-group common cold virus. Proc. Natl. Acad. Sci. USA **91:**1839–1842.
15. **Irie, M.** 1999. Structure-function relationships of acid ribonucleases: lysosomal, vacuolar, and periplasmic enzymes. Pharmacol. Ther. **81:**77–89.
16. **Kowalski, H., I. Maurer-Fogy, G. Vriend, G. Casari, A. Beyer, and D. Blaas.** 1989. Trypsin sensitivity of several human rhinovirus serotypes in their low pH-induced conformation. Virology **171:**611–614.
17. **Laine, P., C. Savolainen, S. Blomqvist, and T. Hovi.** 2005. Phylogenetic analysis of human rhinovirus capsid protein VP1 and 2A protease coding sequences confirms shared genus-like relationships with human enteroviruses. J. Gen. Virol. **86:**697–706.
18. **Lonberg-Holm, K., and B. D. Korant.** 1972. Early interaction of rhinoviruses with host cells. J. Virol. **9:**29–40.
19. **Marlovits, T. C., C. Abrahamsberg, and D. Blaas.** 1998. Very-low-density lipoprotein receptor fragment shed from HeLa cells inhibits human rhinovirus infection. J. Virol. **72:**10246–10250.
20. **Marone, M., S. Mozzetti, D. De Ritis, L. Pierelli, and G. Scambia.** 2001. Semiquantitative RT-PCR analysis to assess the expression levels of multiple transcripts from the same sample. Biol. Proc. Online **3:**19–25.
21. **Nitin, N., P. J. Santangelo, G. Kim, S. Nie, and G. Bao.** 2004. Peptide-linked molecular beacons for efficient delivery and rapid mRNA detection in living cells. Nucleic Acids Res. **32:**e58.
22. **Nurani, G., B. Lindqvist, and J. M. Casasnovas.** 2003. Receptor priming of major group human rhinoviruses for uncoating and entry at mild low-pH environments. J. Virol. **77:**11985–11991.
23. **Prchla, E., E. Kuechler, D. Blaas, and R. Fuchs.** 1994. Uncoating of human rhinovirus serotype 2 from late endosomes. J. Virol. **68:**3713–3723.
24. **Prchla, E., C. Plank, E. Wagner, D. Blaas, and R. Fuchs.** 1995. Virus-mediated release of endosomal content in vitro: different behavior of adenovirus and rhinovirus serotype 2. J. Cell Biol. **131:**111–123.
25. **Rust, R. C., L. Landmann, R. Gosert, B. L. Tang, W. Hong, H. P. Hauri, D. Egger, and K. Bienz.** 2001. Cellular COPII proteins are involved in production of the vesicles that form the poliovirus replication complex. J. Virol. **75:**9808–9818.
26. **Saha, B. K., M. Y. Graham, and D. Schlessinger.** 1979. Acid ribonuclease from HeLa cell lysosomes. J. Biol. Chem. **254:**5951–5957.
27. **Schober, D., P. Kronenberger, E. Prchla, D. Blaas, and R. Fuchs.** 1998. Major and minor receptor group human rhinoviruses penetrate from endosomes by different mechanisms. J. Virol. **72:**1354–1364.
28. **Semler, B. L., and E. Wimmer.** 2002. Molecular biology of picornaviruses. ASM Press, Washington, DC.
29. **Singh, I., and A. Helenius.** 1992. Role of ribosomes in Semliki Forest virus nucleocapsid uncoating. J. Virol. **66:**7049–7058.
30. **Skern, T., C. Neubauer, L. Frasel, P. Grundler, W. Sommergruber, M. Zorn, E. Kuechler, and D. Blaas.** 1987. A neutralizing epitope on human rhinovirus type 2 includes amino acid residues between 153 and 164 of virus capsid protein VP2. J. Gen. Virol. **68:**315–323.
31. **Vlasak, M., M. Roivainen, M. Reithmayer, I. Goesler, P. Laine, L. Snyers, T. Hovi, and D. Blaas.** 2005. The minor receptor group of human rhinovirus (HRV) includes HRV23 and HRV25, but the presence of a lysine in the VP1 HI loop is not sufficient for receptor binding. J. Virol. **79:**7389–7395.